ISSN 0030-400X, Optics and Spectroscopy, 2015, Vol. 119, No. 5, pp. 770–775. © Pleiades Publishing, Ltd., 2015.
Original Russian Text © V.G. Arkhipkin, S.A. Myslivets, 2015, published in Optika i Spektroskopiya, 2015, Vol. 119, No. 5, pp. 745–750.

BASIC PROBLEMS OF OPTICS

Transmission and Reflection Spectra of a Raman Induced Grating in Atomic Media[1]

V. G. Arkhipkin[a, b] and S. A. Myslivets[a, b]

[a] *L.V. Kirensky Institute of Physics, Siberian Branch, Russian Academy of Sciences, Krasnoyarsk, 660036 Russia*
[b] *Siberian Federal University, Krasnoyarsk, 660041 Russia*
e-mail: avg@iph.krasn.ru

Received March 23, 2015

Abstract—The spectral properties of an electromagnetically induced grating that is based on the spatial modulation of the Raman gain in the field of a standing pump wave in a three-level homogeneous medium have been discussed. It has been shown that, by varying the intensity or the frequency of the pump field, one can control the transmission and reflection spectra, while the transmission and reflection coefficients of the probe (Raman) wave can simultaneously be greater than unity. The influence of the nonideality of the standing wave on the spectral characteristics of the grating has been studied.

DOI: 10.1134/S0030400X1511003X

INTRODUCTION

Propagation of light in periodic structures (media) is a field of active research in modern optics with unique possibilities for controlling the propagation of light waves [1]. The optical properties of media with a periodic spatial modulation of the refractive index fundamentally differ from those of homogeneous media. One of the basic properties of these media is the occurrence of bands that are allowed and forbidden for the propagation of light. These structures are known as photonic-crystal structures or photonic crystals [2]. Dynamically controlled periodic structures with the tunable spectral characteristics are of great interest. They can be set up on the basis of electromagnetically induced transparency [3] in the field of a standing controlling wave [4, 5]. As a standing controlling wave interacts with a probe wave in a three level atomic medium, a periodic spatial grating of atomic coherence (an off-diagonal element of the density matrix of a Raman transition) is induced in the medium, which leads to a spatial modulation of the absorption coefficient and nonlinear refractive index for the probe field—an electromagnetically induced absorption grating [6]. Such structures can lead to unusual quantum-optical phenomena. For example, they can give rise to tunable band gaps [4, 7, 8], generation of stationary pulses [9, 10], squeezing of probe pulse [4], tunable reflection (controllable mirror) [11], and light pulse splitting [12].

For controlling light, the Raman interaction of laser fields in atomic media is of great interest [13–15]. Unlike electromagnetically induced transparency, here, the gain rather than the absorption is controlled. In this work, we discuss an alternative scheme for the realization of dynamically tunable periodic structures on the basis of the Raman effect in the field of a standing pump wave, which gives rise to spatially modulated regions with the Raman gain in antinodal regions of the standing wave, i.e., to an induced Raman grating. These gratings can be induced in a three-level atomic medium when a weak Raman (probe) field interacts with a standing pump wave. Particular features of the propagation of the probe wave in this structure and its transmission and reflection spectral characteristics are investigated.

MODEL AND BASIC EQUATIONS

The scheme of the Raman gain is presented in Fig. 1. As a weak probe (Raman) wave at frequency $\omega 2$ interacts with a coherent pump wave at frequency $\omega 1$, it is gained if the frequency difference $\omega 1 - \omega 2$ is close to the frequency of Raman transition $|2\rangle - |0\rangle$. As in the case of spontaneous Raman scattering, gain occurs because the pump energy is transferred to the Raman wave. The intensity of the pump radiation is chosen such that the threshold of the stimulated Raman scattering would not be exceeded, but it should be high enough for the probe wave to be noticeably gained. As distinct from spontaneous Raman scattering, here, as in the case of stimulated Raman scattering, atomic oscillations in the volume occupied by light waves are phased but no uncontrollable instabilities arise. The

[1] VIII International Conference "Basic Problems of Optics" (BPO-2014, October 20–24, 2014, St. Petersburg).

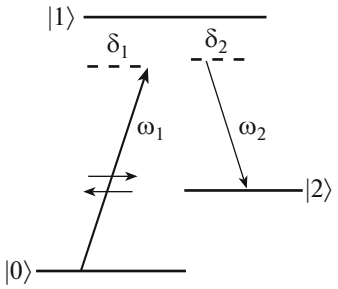

Fig. 1. Scheme of the Raman interaction. Initially, atoms reside in ground state $|0\rangle$. Transitions $|0\rangle$–$|1\rangle$ and $|2\rangle$–$|1\rangle$ are dipole-allowed, while Raman transition $|0\rangle$–$|2\rangle$ is forbidden. Two oppositely directed horizontal arrows indicate that the pumping is a standing wave.

Raman interaction in a three-level medium is described by Raman susceptibility $\chi_R(\omega_2)$ [16]:

$$\chi_R = \frac{1}{4\hbar^3}\frac{|d_{21}|^2|d_{10}|^2}{\delta_1^2(\delta_{20}+i\gamma_{20})}. \quad (1)$$

Here, $\delta_{20} = \delta_1 - \delta_2 = \omega_{20} - (\omega_1 - \omega_2)$ is the Raman detuning, $\delta_{1,2} = \omega_{10,12} - \omega_{1,2}$ is the single-photon detuning, ω_{10} and ω_{12} are the frequencies of the atomic transitions, γ_{20} is the halfwidth of the Raman transition, d_{ij} is the dipole transition matrix element, and $\hbar$ is Planck's constant. Formula (1) is valid for motionless atoms provided that the conditions $|\delta_1| \gg |\Omega_1|, \gamma_{10}$ are fulfilled, where $2\Omega_1 = d_{01}E_1/\hbar$ is the Rabi frequency of the pump field and γ_{10} is the halfwidth of transition $|1\rangle$–$|0\rangle$.

Here, unlike the ordinary Raman interaction, we will assume that the pump wave E_p is a standing wave that is a superposition of two counterpropagating traveling waves $E_p = 1/2\{E_{1+}\exp[-i(\omega_1 t - k_1 z)] + E_{1-}\exp[-i(\omega_1 t + k_1 z)]\}$, where E_{1+} and E_{1-} are the amplitudes of the forward and backward waves, respectively. Then, we will assume that they are real-valued quantities and that $E_{1+} = E_{1-} = E_1$, which corresponds to an ideal standing wave. In this case, $E_p = E_1\exp[-i(\omega_1 t)]\cos(k_1 z)$, and the Rabi frequency of the standing pump wave can be represented as $\Omega_p = 2\Omega_1\cos(k_1 z)$, where $\Omega_1 = d_{01}E_1/2\hbar$. The weak probe wave $E_s = (1/2)E_2\exp[-i(\omega_2 t - k_2 z)]$ ($|E_2| \ll |E_1|$) also propagates along the z axis and interacts with transition $|1\rangle$–$|2\rangle$. In order to obviate absorption, the frequency of the pump field is tuned off the resonant frequency of transition $|1\rangle$–$|0\rangle$. The nonresonant standing wave interacts with the probe traveling wave, which leads to a spatial modulation of the dielectric permittivity due to a Raman nonlinearity. The dielectric permittivity for the Raman wave has the form

$$\begin{aligned}\varepsilon_2(z) &= 1 + 4\pi N\chi_2 + 4\pi N\chi_R|E_1|^2\cos^2(k_1 z)\\ &= \varepsilon_{20} + \Delta\varepsilon(1+\cos(2k_1 z)),\end{aligned} \quad (2)$$

where

$$\Delta\varepsilon = 2\pi\chi_R N|E_1|^2 = \frac{4\pi|d_{21}|^2 N}{\delta_1^2(\delta_{20}+i\gamma_{20})}\Omega_1^2\cos^2(k_1 z),$$

$\varepsilon_{20} = 1 + 4\pi N\chi_2$, χ_2 is the off-resonant linear susceptibility for the probe field, and N is the atomic concentration.

The dielectric permittivity is periodically modulated in space as $\cos(2k_1 z)$ due to the standing pump wave. Physically, this is caused by the fact that a grating of atomic coherence is induced for Raman transition $|0\rangle$–$|2\rangle$ (off-diagonal element of the density matrix). This leads to a spatial modulation of the gain coefficient and refractive index (at $\delta_{20} \neq 0$). Gain occurs in antinodal regions of the standing pump wave. We call this structure the electrodynamically induced Raman grating. Due to the spatial modulation, a weak probe wave propagates in the medium as in a one-dimensional grating with a spatial period $\lambda_1/2$, where λ_1 is the wavelength of the pump radiation. Under these conditions, the probe wave propagates not only forward, but also backward; i.e., a reflected Raman wave arises.

Upon normal incidence, the wave equation for $E_2(z)$ in a medium with a spatially modulated dielectric permittivity has the form [17]

$$\frac{d^2E_2}{dz^2} + k_{20}^2\varepsilon_2(z)E_2 = 0. \quad (3)$$

Taking into account (2), Eq. (3) takes the form

$$\frac{d^2E_2}{dz^2} + k_2^2[1+\beta(1+\cos 2k_1 z)]E_2 = 0, \quad (4)$$

where $k_{20} = \omega_2/c$, $k_2^2 = k_{20}^2\varepsilon_{20}$, and $\beta = \Delta\varepsilon/\varepsilon_{20}$.

Using the coupled waves method [18], the solution of Eq. (4) can be represented as a superposition of two counterpropagating waves:

$$E_2(z) = A(z)e^{ik_2 z} + B(z)e^{-ik_2 z}, \quad (5)$$

where $A(z)$ and $B(z)$ are the amplitudes of the forward and backward waves, respectively. Substituting (5) into (4) and using the slowly varying amplitudes approximation ($d^2E_2/dz^2 \ll k_2 dE_2/dz$), we obtain a system of two coupled equations for $A(z)$ and $B(z)$,

$$\frac{dA}{dz} = i\alpha A + i\sigma Be^{i2\Delta k z}, \quad \frac{dB}{dz} = -i\alpha B - i\sigma Ae^{-i2\Delta k z}, \quad (6)$$

where $\alpha = k_2\beta/2$, $\sigma = k_2\beta/4$, and $\Delta k = k_1 - k_2$.

Linearly independent solutions of system (6) are proportional to $\exp(\pm isz)$, where $s = \sqrt{(\Delta k - \alpha)^2 - \sigma^2}$, while amplitudes $A(z)$ and $B(z)$ prove to be modulated with spatial frequency s,

$$A(z) = e^{ik_1 z}(a_1 e^{isz} + a_2 e^{-isz}), \quad (7)$$

$$B(z) = e^{-ik_1 z}(b_1 e^{-isz} + b_2 e^{isz}), \quad (8)$$

$$\kappa(\omega_2) = k_1 \pm \sqrt{(\Delta k - \alpha)^2 - \sigma^2} = k_1 \pm s. \quad (9)$$

Here, $a_{1,2}$ and $b_{1,2}$ are constants of integration, which are determined by the boundary conditions, while expression (9) for $\kappa(\omega_2)$ is the dispersion relation. Formulas (7) and (8) define linearly independent solutions or normal waves in the approximation $|\Delta\varepsilon| \ll 1$ (small modulation depth) and $|\Delta k| \ll |k_2|$. Therefore, forward and backward probe waves are superpositions of two spatial harmonics, which can interfere.

In order to determine constants of integration in formulas (7) and (8), we set boundary conditions from the following considerations. Since $|\Delta\varepsilon| \ll 1$, we can neglect the Fresnel reflection from boundary layers and take into account only the volume reflection. In this case, the boundary conditions take the form of those for the perfectly matched layer of thickness L [18]: $A(z = 0) = A_0$, $B(z = L) = 0$, where A_0 is the amplitude of the incident probe wave. With these boundary conditions, the solutions of (7) and (8) can be represented as

$$A(z) = A_0[s\cos s(L-z) + i(\Delta k - \alpha)\sin s(L-z)]/D, \quad (10)$$

$$B(z) = A_0\sigma \sin s(L-z)/D, \quad (11)$$

where $D = s\cos(sL) + i(\Delta k - \alpha)\sin(sL)$, and L is the length of the specimen.

We will introduce the notation $t(z) = A(z)/A_0$ and $r(z) = B(z)/A_0$. Using (10) and (11), we obtain

$$t(z) = \frac{s\cos s(L-z) + i(\Delta k - \alpha)\sin s(L-z)}{s\cos(sL) + i(\Delta k - \alpha)\sin(sL)}, \quad (12)$$

$$r(z) = \frac{\sigma \sin s(L-z)}{s\cos(sL) + i(\Delta k - \alpha)\sin(sL)}. \quad (13)$$

Correspondingly, the energy transmission and reflection coefficients $T = |A(z = L)/A_0|^2$ and $R = |B(z = 0)/A_0|^2$ can be written as $T = |t(z = L)|^2$ and $R = |r(z = 0)|^2$.

RESULTS AND DISCUSSION

For numerical calculations, we will use parameters that correspond to the $D1$ line of motionless Na atoms. Transition $|0\rangle$–$|2\rangle$ corresponds to a hyperfine splitting of the ground state $3S_{1/2}$, $\gamma_{10} = 2\pi \times 10$ MHz, $\gamma_{20} = \gamma_{10}/100$, and $N = 10^{12}$ cm^{-3}. Then, Rabi frequencies of the pump field will be expressed in units of γ_{10}, while the Raman detuning will be expressed in units of γ_{20}.

Figure 2a shows typical dependences of $\mathrm{Im}(\kappa(\omega_2)) = \mathrm{Im}(s(\omega_2))$ and $\mathrm{Re}(s(\omega_2))$ as functions of the Raman detuning for Rabi frequency of the pump field $\Omega_1 = \gamma_{10}$. Qualitatively, the behavior of Ims and Res does not depend on the magnitude of the intensity of the pump field. In the range $\delta_{20} < 0$, Im$s > 0$, while $\mathrm{Im}(-s) < 0$. At $\delta_{20} > 0$, the contrary is the case. Upon passage through the resonance, a jump takes place. Figures 2b, 2c, and 2d present dependences of the intensities of the forward and backward probe waves in a specimen with a length of $L = 500\lambda_1$ as functions of the normalized coordinate z/L. Their behavior at a given length of the specimen, strongly depends on the Raman detuning and the intensity of the pump field. It is seen that the forward and backward waves in the specimen are inhomogeneous; i.e., they can either be gained or decay.

We will represent the complex amplitudes of the spatial harmonics for forward wave (7) as $a_{1,2} = A_{1,2}\exp(i\varphi_{1,2})$, where $A_{1,2}$ are the real-valued amplitudes and $\varphi_{1,2}$ are the phases. Figure 3 shows the spatial distributions of real amplitudes $A_{1,2}$ and phases $\varphi_{1,2}$ of forward wave $A(z)$ inside of the specimen for differ-

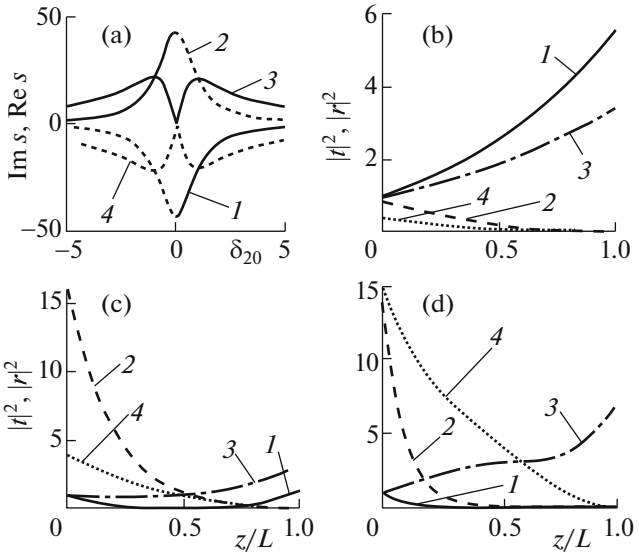

Fig. 2. (a) Imaginary (*1*, *2*) and real (*3*, *4*) parts of $\pm s$ as functions of the Raman detuning δ_{20} (in units of γ_{20}). (b, c, d) Spatial distributions of the normalized intensity for the (*1*, *3*) forward ($|t|^2$) and (*2*, *4*) backward ($|r|^2$) waves in the specimen at different values of the Rabi frequency Ω_1 of the pump field and Raman detuning δ_{20}: (b) $\Omega_1 = 0.5\gamma_{10}$, $\delta_{20} =$ (*1*, *2*) 0 and (*3*, *4*) $0.5\gamma_{20}$; (c) $\Omega_1 = \gamma_{10}$, $\delta_{20} =$ (*1*, *2*) 0 and (*3*, *4*) $0.95\gamma_{20}$; and (d) $\Omega_1 = 1.5\gamma_{10}$, $\delta_{20} =$ (*1*, *2*) 0 and (*3*, *4*) $1.6\gamma_{20}$.

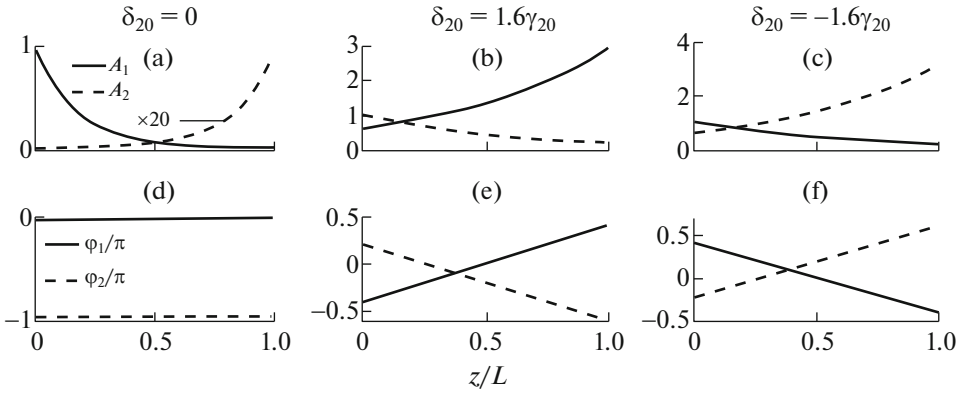

Fig. 3. Dependences of normalized real amplitudes $A_{1,2}/A_0$ and phases $\varphi_{1,2}/\pi$ on the coordinate z/L inside of a specimen for frequency detunings $\delta_{20} = 0$ and $\delta_{20} = \pm 1.6\gamma_{20}$, which correspond to transmission peaks at $\Omega_1 = 1.5\gamma_{10}$.

ent values of the Raman detuning δ_{20}. It is seen (a, b, c) that one of the harmonics is gained, while the other harmonic decays; it is also seen (d, c, f) that they can be either in phase or out of the phase; i.e., they can interfere either constructively or destructively.

Figures 4a and 4b show the transmission and reflection spectra as functions of the Raman detuning for different values of Rabi frequency Ω_1 of the pump field. Here, we fix single-photon detuning δ_1 of the pump field and vary δ_2. It can be seen that the transmitted and reflected fields can be simultaneously gained in a certain frequency range, which depends on the intensity of the pump field. Therefore, the transmission coefficient may be interpreted as a gain coefficient. At weak pump fields, the transmitted and reflected signals have maximal amplitude, which correspond to the Raman resonance frequency. As the pump intensity increases, a dip in the transmission spectrum arises, the depth and width of which increase as the pump intensity further increases. A similar pattern is observed for the reflection, but the dip arises here at a higher pump intensity than in the case of the transmission In the range between the peaks, the transmission tends to zero, whereas the reflection coefficient remains to be greater than unity. Far from the Raman resonance, $T \to 1$ and $R \to 0$; i.e., the specimen becomes transparent.

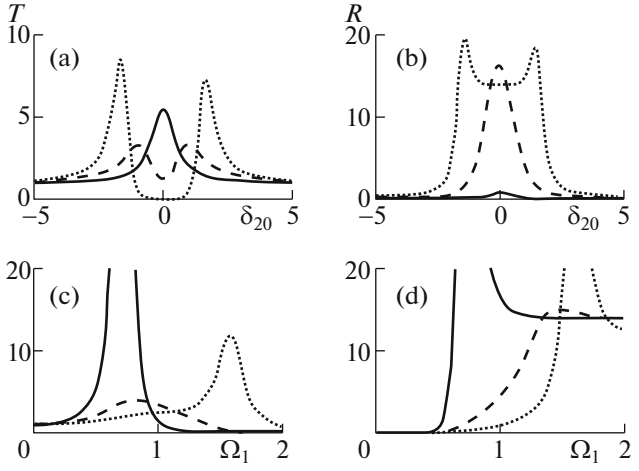

Fig. 4. (a, b) Dependences of transmission and reflection coefficients T and R on the Raman detuning δ_{20} at different values of the Rabi frequency Ω_1 (in units of γ_{10}): (solid curve) 0.5, (dashed curve) 1, and (dotted curve) 1.5. (c, d) Dependences of T and R on Rabi frequency Ω_1 of the pump field at different values of the Raman detuning δ_{20} (in units of γ_{20}): (solid curve) 0.5, (dashed curve) 0.95, and (dotted curve) 1.6.

Figures 4c and 4d present the dependences of the transmission and reflection coefficients on Rabi frequency Ω_1 of the pump field at different values of the Raman detuning. The transmission and reflection increase with increasing intensity of the pump field as long as it exceeds a certain threshold value (subthreshold regime). Above this threshold, the transmission decreases (down to zero) with increasing pump intensity (superthreshold regime).

Figures 5a and 5b show, respectively, the transmission and reflection coefficients as functions of Ω_1 and δ_{20}, with positions of transmission and reflection peaks being indicated.

Up to now, we have assumed that the standing pump wave is ideal. In this case, the pump intensity varies periodically from 0 (at nodes) to a maximal value $4E_1^2$ (at antinodes). Atoms that are located at nodes do not gain the probe radiation. Under real conditions, the standing wave is not ideal, because the amplitudes of the counterpropagating waves are not equal to each other. As a result, the pump field at nodes differs from zero (quasi-nodes), while its maximum value at antinodes is smaller than that for the

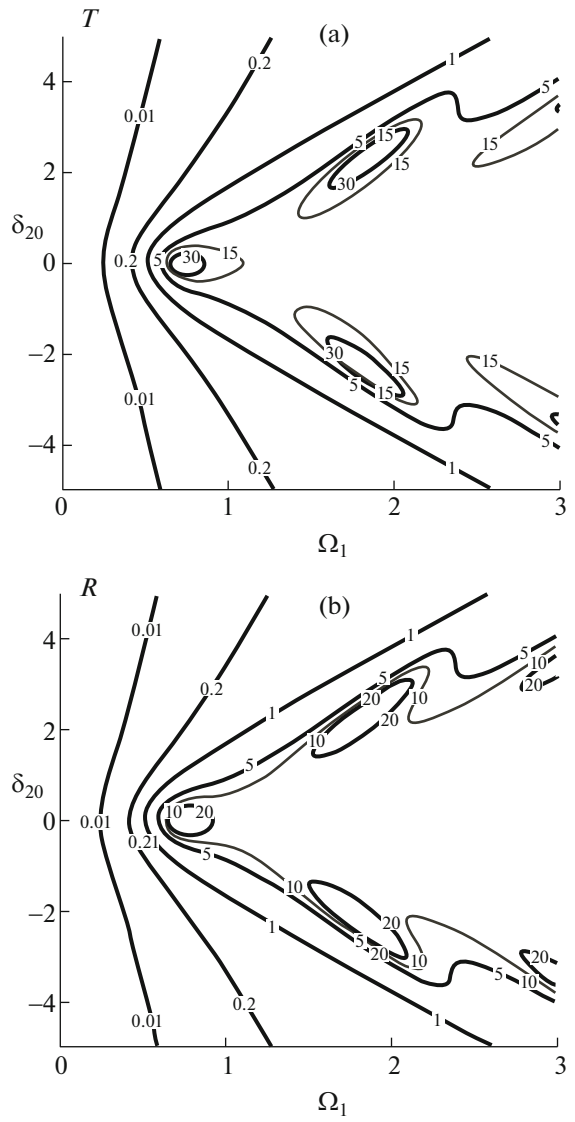

Fig. 5. Patterns of the transmission and reflection coefficients T and R in the plane Ω_1 and δ_{20}. Numerals near curves correspond to values of the transmission and reflection coefficients.

ideal standing wave. Therefore, the Raman gain takes place here at quasi-nodes as well; but the contrast in the grating decreases. In this case, formula (2) for the dielectric permittivity can be represented as

$$\varepsilon_2(z) = \varepsilon_{20} + \Delta\varepsilon[1 + p\cos(2k_1 z)],$$

$$\Delta\varepsilon = 2\pi\chi_R N(E_{1+}^2 + E_{1-}^2) = 2\pi\chi_R N E_{1+}^2(1 + a^2),$$

$$p = 2E_{1+}E_{1-}/(E_{1+}^2 + E_{1-}^2) = 2a/(1+a^2),\ \ a = E_{1-}/E_{1+}.$$

Figure 6 shows the dependences of the transmission and reflection coefficients that are similar to those presented in Fig. 4, but that were determined at different values of parameter a. Here, solid curves correspond to the case of an ideal standing pump wave

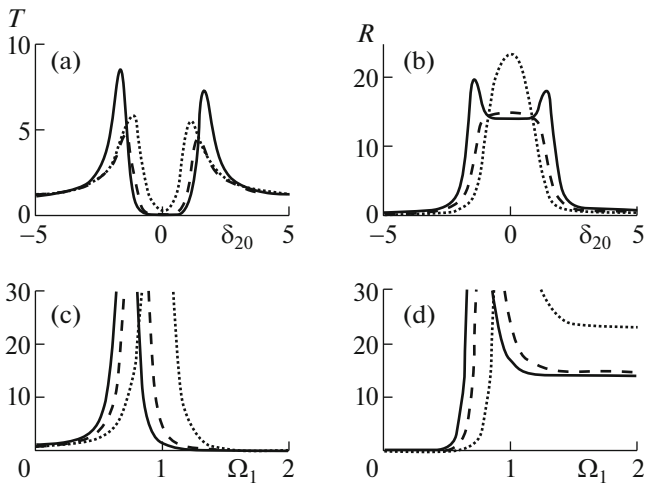

Fig. 6. (a, b) Transmission and reflection spectra T and R as functions of Raman detuning δ_{20} at $\Omega_1 = 1.5\gamma_{10}$ and (c, d) dependences of T and R on Rabi frequency Ω_1 of the pump field under the Raman resonance conditions $\delta_{20} = 0$ for the values of the parameter a equal to (solid curve) 1, (dashed curve) 0.8, and (dotted curve) 0.5.

($a = 1$). It is seen that these dependences are not too sensitive to the value of a. Using large values of the intensity of the pump field, one can obtain characteristics that are close to the case of an ideal standing wave.

CONCLUSIONS

We have theoretically studied the spectral properties of an electrodynamically induced grating that is based on the Raman interaction of a probe wave with a standing pump wave in atomic media assuming that atoms are motionless. In contrast to electrodynamically induced absorption gratings, which are based on the electromagnetically induced transparency, here, the gain rather than the absorption is controlled. This scheme also differs from the scheme of a Bragg grating with fixed parameters in distributed feedback lasers, where the linear dielectric permittivity is modulated. We showed that the transmission and reflection coefficients can both be simultaneously greater than unity in a certain frequency range, while the transmission and reflection spectra can be dynamically controlled by varying the intensity or the frequency of the pump field. At certain intensities of the pump field, the transmission can be close to zero, and small changes in the intensity can transfer the system from the transparent to an opaque state. This controllable transmission may be of interest for optical switching. The necessary pump intensity depends on the single-photon detuning of the pump field, the width of the Raman resonance, the length of the medium, etc. and can be 1–100 mW/cm^2 or lower. The obtained results agree

well with exact calculations based on recurrence relations [19].

To experimentally realize the scheme, cold atoms can be used. The possibility of using hot atoms requires additional investigations. Among solid-state materials, praseodymium-doped Y_2SiO_5 crystals and *NV*-centers in diamonds, which have Raman transitions with long-lived coherency, are of interest.

ACKNOWLEDGMENTS

This work was supported by the Russian Foundation for Basic Research, project no. 15-02-03959.

REFERENCES

1. *Nonlinearities in Periodic Structures and Metamaterials*, Ed. by C. Denz, S. Flach, and Yu. Kivshar (Springer-Verlag, 2009).
2. J. D. Joannopoulos, S. G. Johnson, J. N. Winn, and R. D. Meade, *Photonic Crystals: Molding the Flow of Light* (Princeton Univ. Press, Princeton, 2008).
3. M. Fleischhauer, A. Imamoglu, and J. P. Marangos, Rev. Mod. Phys. **77**, 633 (2005).
4. B. S. Ham, Phys. Rev. A **71**, 013821 (2005).
5. J.-H. Wu, A. Raczynski, J. Zaremba, et al., J. Mod. Opt. **56**, 768 (2009).
6. A. W. Brown and M. Xiao, Opt. Lett. **30**, 699 (2005).
7. A. Andre and M. D. Lukin, Phys. Rev. Lett. **89**, 143602 (2006).
8. M. Artoni, Phys. Rev. Lett. **96**, 073905 (2006).
9. M. Bajcsy, A. S. Zibrov, and M. D. Lukin, Nature **426**, 638 (2003).
10. S. A. Moiseev, A. I. Sidorova, and B. S. Ham, Phys. Rev. A **89**, 043802 (2014).
11. X.-J. Zhang, H. H. Wang et al., J. Opt. Soc. Am. B **30**, 1905 (2013).
12. Y. Xue and B. S. Ham, Phys. Rev. A **78**, 053830 (2014).
13. K. J. Jiang, L. Deng, and M. G. Payne, Phys. Rev. A **74**, 041803 (2006).
14. K. J. Jiang, L. Deng, and M. G. Payne, Phys. Rev. A **76**, 033819 (2007).
15. N. I. Shamrov, Opt. Spectrosc. **105** (4), 566 (2008).
16. S. A. Akhmanov and N. I. Koroteev, *Methods of Nonlinear Optics in Spectroscopy of Light Scattering* (Nauka, Moscow, 1981) [in Russian].
17. S. G. Rautian, Opt. Spectrosc.**104** (1), 112 (2008).
18. S. Yu. Karpov and S. N. Stolyarov, Usp. Fiz. Nauk **163**, 64 (1993).
19. V. G. Arkhipkin and S. A. Myslivets, Quantum Electron. **39** (2), 157 (2009).